

**ABSOLUTE FRAGMENTATION CROSS SECTION MEASUREMENTS
OF SMALL MOLECULES INDUCED BY H⁺ AND N⁺ ION IMPACT****S.T.S. Kovács^{1,2}, P. Herczku^{1,2}, L. Gulyás¹, Z. Juhász¹, B. Sulik¹**¹MTA Institute for Nuclear Research, 4026 Debrecen, Bemtér 18/c²University of Debrecen, 4032 Debrecen, Egyetem tér 1.**Abstract**

Ion induced fragmentation of small molecules was investigated by the impact of 650 keV N⁺ and 1 MeV H⁺ projectiles. The measured fragment ion and electron emission spectra were converted into absolute double differential cross sections. The absolute electron emission cross sections obtained for 1 MeV H⁺ + CH₄ collision are in good agreement with those of D. J. Lynch et al. (J. Chem. Phys. 64, 2616 (1976)) and with our CDW-EIS calculations. The fragment ion spectra of CH₄ target are compared for H⁺ and N⁺ projectiles.

I. Introduction

Fragmentation of small molecules have been extensively studied with photon [1, 2], electron [3, 4], and ion [5-7] impact on various types of simple molecules. Because of their fundamental and practical importance H₂, N₂, CO, CO₂, H₂O and CH₄ are the most frequently investigated target molecules. Water is the main constituent in living cells. The methane molecule is the simplest hydrocarbon molecule and a monomer of several larger hydrocarbons. Both molecules are important for living organisms, therefore they are used as tissue-equivalent materials in radiological studies [8].

The primary lesions of the tissue which finally lead to cell death occur on atomic and molecular dimensions. When a charge particle collides with a molecule, energy is transferred to it. Due to this energy transfer a (transient)

molecular ion can be formed through excitation and ionization processes. This molecular ion than may dissociate with a certain probability into two or more fragments. The energy and charge state of the emergent fragments reveals to the fragmentation channel in which the fragment has been produced. From the fragment ion energy spectra we can deduce among others the charge state distribution of the transient molecular ions, and the cross sections for the target multiple ionization channels which lead to the dissociation of the molecule.

In this work, we determine absolute double differential cross sections for both the ionization process and the emission of ionic fragments. Absolute cross sections are characteristic for the given collision system. They are directly comparable with theories. They are independent from the experimental parameters (target density, beam current, detection efficiency etc.). Accordingly, these parameters should be accurately known to extract absolute cross sections from the measured yields.

Absolute ionization and fragmentation cross sections are important not only for fundamental understanding, but they provide valuable input data for complex ion-matter interaction models, e.g., for those of irradiation dose calculations for radiotherapy treatments [9].

II. Experiment

In this work we investigated the dissociation of small molecules at the beam line of the VdG-5 electrostatic accelerator in Atomki. The experimental arrangement was described in Ref. [10] and [11] therefore we give only a brief survey here.

Molecule fragmentation experiments were carried out on gas phase H₂O and CH₄ targets by the impact of 650 keV N⁺ and 1 MeV H⁺ projectiles. The target molecules were injected into the collision region through a nozzle [12]. The ion beam was carefully collimated to the size of 2x2 mm. After it passed through the collision volume, the beam current was measured in a two-stage Faraday cup. The energy/charge ratio of the ejected fragments was measured by an energy dispersive electrostatic spectrometer designed specifically for molecule fragmentation experiments [13].

The pressure in the experimental chamber was typically a few times 10⁻⁵ and less than 2·10⁻⁶ mbar with and without target gas injection respectively. The beam current was in the order of 100 nA for the H⁺ and around 20 nA for the N⁺ projectile.

III. Data evaluation

We determine absolute double differential cross sections for both fragmentation (fig. 1) and electron emission (fig 2). The double differential cross section (DDCS) for particle emission by particle impact is expressed by the measured quantities and the experimental parameters as follows.

$$\frac{d^2\sigma}{d\Omega dE} = \frac{n}{N \cdot \rho \cdot l \cdot \Delta\beta \cdot \eta \cdot r \cdot E} \quad (1)$$

Here n is the measured counts, N is the number of particles in the beam, ρ is the target density in the collision volume, l is the effective target length along the projectile ion beam, $\Delta\beta$ is the (receptive) solid angle of the spectrometer, η is the detection efficiency, $r = \Delta E/E$ is the energy resolution of the analyzer and E is the selected energy of the charged particles.

For ion impact, the number of particles in the beam can be determined e.g., by measuring the current in a Farady-cup. It reads.

$$N = \frac{Q}{q e} \quad (2)$$

Here Q is the collected charge, which is an integral of the beam current over the time of data collection at a given angle and energy. In the denominator, q is the charge state of the projectile ion, and e is the elementary charge.

In our experiments, the beam current was measured in a two-staged faraday cup. The collected charge (Q) was integrated and digitalized by a current integrator. The integrated charge was saved in the data file in every two seconds together with the corresponding collected counts (n) in the detector.

The density of the target gas in the collision volume was estimated from the parameters of the gas target system [12]. From the measured gas pressure in the puffer container and the geometrical parameters of the elements of the gas inlet system including the nozzle, we calculated the flow resistance, the pressure drop and finally the pressure and target density at the exit of the nozzle. Taking into account the gas expansion we made estimations for the gas flow profiles according to data from literature [14]. The target molecule density in the

collision volume was found to be a few times 10^{13} molecule/cm³ for the applied puffer pressure region of 10-35 mbar.

The effective target length (l) and the receptive solid angle of the spectrometer ($\Delta\beta$) were calculated from the geometry of the collision volume and the geometrical data of the spectrometer. In an ideal case the target would have a cylindrical shape with homogeneous gas density distribution in it, and the spectrometer would receive particles from the whole collision volume (it would "see" the whole collision volume). In reality the target gas profile has more a conical-like shape, and the target gas density decreases with the increasing distance from the central axis of the cone. At the observation angle of 90° the effective target length is l_0 . Rotating the spectrometer toward higher or lower angles l is increasing. If we assume that the gas density is homogenous, we need a correction of $1/\sin\theta$ for the target length (where θ is the observation angle). Taking into account the inhomogeneity of the gas jet target, the correction will have the form [15]:

$$l = l_0 \frac{1}{c+(1-c) \sin \theta} \quad (3)$$

The constant c accounts for the density distribution of the target ($c=0$ represents a homogenous target, while $c=1$ belongs to an ideal, cylindrical jet target with small diameter). With other words, the complex density distribution of the real target is approximated by a linear combination of two simple extremes. In our case this approximation works very well for all studied collision systems, with $c=0.8$.

The effective solid angle, under which the ejected particles from a point of the target volume enter into the analyzer was: $\Delta\beta=0.001$ sr.

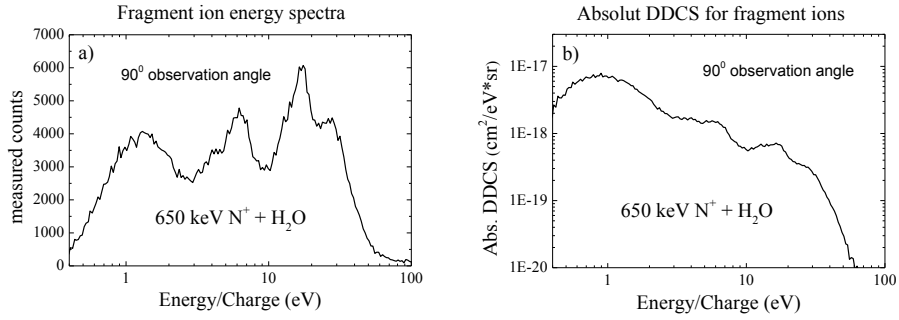


Figure 1: Measured fragment ion energy spectra at the observation angle of 90° (a), and the same spectra converted to absolute scale (b).

The detection efficiency (η) is determined by many factors. The most important are the efficiency of the channeltron detector, the transparency of the mesh placed in front of the detector, the fringe field effects at the slits and the signal recognition efficiency of the electronics. For our spectrometer, the total detection efficiency is estimated to be 50%. The energy resolution (r) is determined by the properties of the energy analyzer of the spectrometer. It is 3% for our system.

With the above method we determined the absolute fragmentation (figure 1) and electron emission (figure 2) cross sections from the measured spectra. The obtained absolute electron emission spectra for the collision of 1 MeV H⁺+CH₄ are in good agreement with those of D. J. Lynch et al, and with our CDW-EIS calculations (comparison is shown in figure 2).

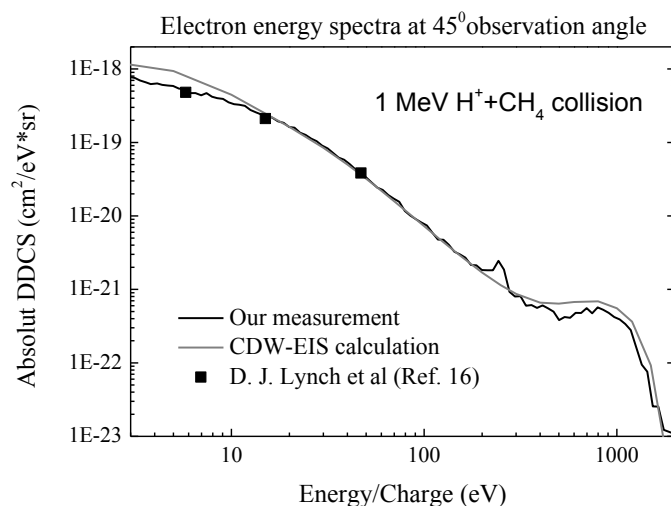


Figure 2: Comparison of our measured electron emission spectra at the observation angle of 45° with those of in Ref. 16 and with our CDW-EIS calculations.

The agreement with the earlier experimental reference data is remarkable. It shows that our experimental arrangement is highly under control, we know its details and the values of its parameters very well. The agreement with CDW-EIS theory is a topic of a forthcoming paper, here we only demonstrate that collision systems at a low perturbation level are well understood nowadays. The present frontiers in ion-molecule collisions are located at stronger perturbations, especially by the impact of dressed projectiles.

Results and discussions

Three main structures appear in the spectra for both projectiles (see figure 3). A region below 2.5 eV contains mostly heavy fragments from all of the fragmentation channels (unresolved), and some additional H^+ (maybe also H_2^+) fragment contribution from ion-neutral dissociation channels. The structures between 2.5-3.7 eV are mostly due to H_2^+ fragments, also with some single ionization contribution. Above ~ 4 eV the structures are identified as protons originating from the different fragmentation channels of CH_4 . The energy of

the fragments increases with the increasing Coulomb repulsion between the charged fragments. Accordingly, the energy of the H^+ fragment carries the information about the fragmentation channel and, in turn, the degree of ionization of its parent molecular ion.

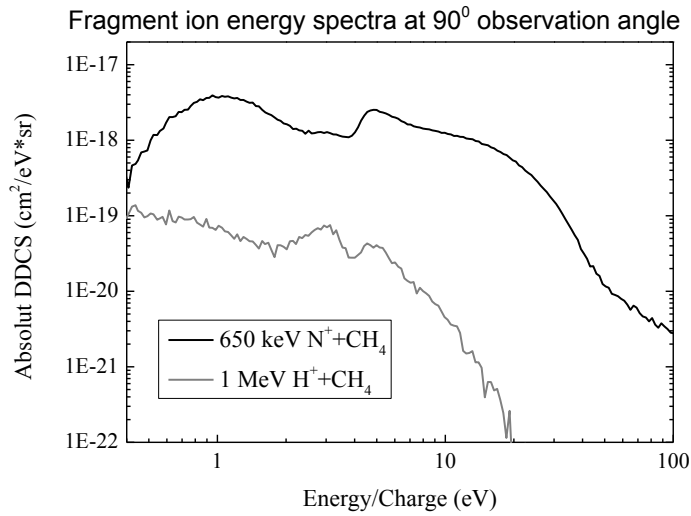


Figure 3: Comparison of the spectra of CH_4 fragment ions for H^+ and N^+ projectiles.

The main differences between the fragmentation spectra for H^+ and N^+ projectiles are as follows. The yield for N^+ is significantly higher at all fragment energies than for H^+ projectile. Above 10 eV where multiple (three- and fourfold) ionization dominates the N^+ projectile is much more effective than the H^+ one. Finally, the relative yields of the different fragmentation channels differ for the two types of projectiles not only in magnitude, not only in tendency, but also in local structures.

An analysis of the fragmentation channels shows that in the case of proton projectile, the maximal ionization degree of the methane molecule is $q=2$, while for N^+ projectile it is $q=4$. This difference is attributed to the stronger perturbation of the N^+ ion. If we characterize the interaction strength with the Sommerfeld parameter ($k=Q/v$) [17] we find the 650 keV N^+ projectile about four times more perturbative ($k=0.73$) than that for the 1 MeV H^+ projectile

($k=0.16$). This is valid in distant collision conditions where the projectile electrons properly screen, and only the field of the ionic charge perturbs the target system. If we also consider the close collision events for “dressed up” projectiles, their effective charge there may highly exceed the ionic value [18]. As an extreme, the Sommerfeld parameter has a huge value, $k=5.14$ for 650 keV bare N^{7+} ion. One might imagine the effect that for a short time, while the electron clouds overlap, the screening of the projectile electrons drastically decreases. Accordingly, the target electrons feel a short but strong, abrupt pull [19], which is likely to create high degrees of multiple ionization of the CH_4 molecule.

Detailed evaluation and interpretation of the measured data are in progress.

Work was supported by the Hungarian OTKA Grant nos. K73703 and K109440, and by the TAMOP4.2.2.A-11/1/KONV-2012-0036 projects, which are co-financed by the EU and the European Social Fund.

References

- [1] H. B. Pedersen et al, Phys. Rev. **A87**, 013402 (2013).
- [2] G. Dujardin et al, Phys. Rev. A **31**, 3027 (1985).
- [3] A. L. F. de Barros et al, Phys. Rev. **A80**, 012716 (2009).
- [4] F. Frémont et al, Phys. Rev. A **72**, 042702 (2005).
- [5] H. Luna et al, Phys. Rev. A **75**, 042711 (2007).
- [6] U. Werner et al, NIM B **98**, 385 (1995).
- [7] F. Alvarado et al, J. Phys. **B38**, 4085 (2005).
- [8] I. Baccarelli et al, Eur. Phys. J. D **60**, 1-10 (2010).
- [9] A. V. Solov'yov et al, Phys. Rev. E **79**, 011909 (2009).
- [10] S. T. S. Kovács et al, Act. Phys. Deb. **XLVI**, 65 (2012).
- [11] S. T. S. Kovács et al, ATOMKI Annual Report 2010 57 (2011).
- [12] S. T. S. Kovács, ATOMKI Annual Report 2010 56 (2011).
- [13] P. Herczku, ATOMKI Annual Report 2010 55 (2011).

- [14] S. Bohátka, Vákuumfizikaés –technika, (2008).
- [15] E. Lattouf et al, Phys. Rev. A **89**, 062721 (2014).
- [16] D. J. Lynch et al, J. Chem. Phys. **64**, 2616 (1976).
- [17] B. Siegmann et al, Phys.Rev. A **62**, 022718 (2000).
- [18] S. T. S. Kovács et al, Act. Phys. Deb. **XLVII**, 87 (2013).
- [19] L. Sarkadi et al, Phys. Rev. A **87**, 062705 (2013).